Enhanced photocatalytic nitrogen fixation on defects regulated Ni-doped MIL-101(Fe) via nitrogen coordinated activation

Lu Liu [a, b], Bingqian Hu [a, b], Qi Chen [a, b], Zefeng Yang [a, b], Yueling Chen [a, b], Jionghua Wu [a, c, *], Jimmy C. Yu [a, b, d], Ling Wu [a, b, *]

[a] State Key Laboratory of Chemistry for NBC Hazards Protection, College of Chemistry, Fuzhou University, Fuzhou 350116, China

[b] State Key Laboratory of Photocatalysis on Energy and Environment, College of Chemistry, Fuzhou University, Fuzhou 350116, China

[c] Institute of Micro-Nano Devices and Solar Cells, College of Physics and Information Engineering, Fuzhou University, Fuzhou 350116, China

[d] Department of Chemistry, Chinese University of Hong Kong, Shatin, New Territories, Hong Kong 999077, China

* Corresponding authors

E-mail address: JionghuaWu@fzu.edu.cn (J. Wu), wuling@fzu.edu.cn (L. Wu).

Supplementary Information

1.1. Materials.

All of the chemicals were of analytical grade and utilized without undergoing additional purification. Iron chloride hexahydrate ($FeCl_3 \cdot 6H_2O$, 99%) , N, N-dimethylformamide (DMF, AR) and ethanol (≥99.8%)were acquired from Sinopharm Chemical Reagent Co. Hexahydrate nickel chloride ($NiCl_2 \cdot 6H_2O$, 99%) from Shanghai Titan Technology Co., Ltd. terephthalic acid (H_2BDC, 99%) was obtained from Thermo scientific Co., Ltd.

1.2. Synthesis of MIL-101(Fe) and MIL-101(Fe/Ni)-X%

MIL-101(Fe) was produced through a solvothermal method based on the previous protocol with minor modifications [65]. In short, 20 mL of DMF containing 0.206 g (1.24 mmol) of terephthalic acid was mixed with 0.675 g (2.5 mmol) of $FeCl_3 \cdot 6H_2O$. The yellow mixture was moved to a 25 mL autoclave lined with Teflon and heated to 110°C for 20 h after being stirred for 20 minutes. The product was collected by centrifugation after being cooled to room temperature and then washed six times with DMF and ethanol. The product was dried overnight in a vacuum oven to obtain reddish-brown powder. Finally, the products were treated to 150°C for 2 h in a vacuum oven. Samples with different Ni^{2+} doping ratios were synthesized through the same process, with molar ratios of $FeCl_3 \cdot 6H_2O$/$NiCl_2 \cdot 6H_2O$ (0.95/0.05, 0.90/0.10, 0.85/0.15, and 0.80/0.20). The obtained samples were denoted as MIL-101(Fe/Ni)-5%, MIL-101(Fe/Ni)-10%, MIL-101(Fe/Ni)-15%, and MIL-101(Fe/Ni)-20%, respectively. The actual nickel content in the synthesized samples was measured employing inductively coupled plasma optical emission spectroscopy (ICP-OES). As seen in Table S1, the real nickel amount of MIL-101(Fe), MIL-101(Fe/Ni)-5%, MIL-101(Fe/Ni)-10%, MIL-101(Fe/Ni)-15%, and MIL-101(Fe/Ni)-20% is 0%, 3%, 6%, 11%, and 14%, slightly lower than the theoretical doping levels.

1.3. Performance Testing of Photocatalytic Nitrogen Fixation

In a quartz container, 20 mg of the product were distributed in 20 ml of ultrapure water. Then ultrapure nitrogen was bubbled into the container at an average rate of 18 mL/min under dark for 0.5h. Subsequently, under the irradiation of a xenon lamp (300W) equipped with a cut off filter (λ>400 nm), the reactor underwent a reaction of photocatalytic nitrogen fixation. Following the reaction, the filtrate is obtained by filtering the suspension via a syringe fitted with a membrane filter (0.22 μm). Cation exchange chromatography was then used to measure the filtrate's NH_4^+ concentration (column: SH-CC-3L; column temperature: 35°C; flow rate: 1 mL/min; pressure: 7 MPa). Fig. S1 displays the NH_4^+ standard curve.

1.4. Analysis of Oxygen-Producing Experiments

To measure O_2 production, 20 mg of MIL-101(Fe/Ni)-X% was weighed and introduced to a reactor with 20 mL of ultrapure water. To remove dissolved O_2 from the solution, high-purity nitrogen gas was continuously purged in the reactor for 30 min in the absence of light. The container was sealed in darkness with the flask filled with N_2. Substances extracted from the reactor prior to illumination showed only nitrogen signals was detected by gas chromatography. After that, a 300W xenon lamp (λ > 400 nm) was used to irradiate the suspension. Gas chromatography (Agilent GC-7890B) was used to detect O_2 content over reaction times ranging from 1 to 8 hours.

1.5. Time-depend in-situ DRIFTS measurement

We employed in situ diffuse infrared Fourier transform spectroscopy (DRIFTS) measurements over time employing an FTIR spectrometer (Nicolet IS50) equipped with a Harrick in-situ diffuse reflectance cell. Firstly, the powdered sample was compacted and placed in a custom-made infrared reaction chamber. Secondly, 99.999% pure Ar gas was introduced to desorb adsorbed gases from the catalyst, followed by

heating at a rate of 5°C/min to 150°C and holding at this temperature for 2 hours. Thirdly, to determine the N_2 adsorption level, a background spectrum was acquired upon cooling to room temperature. Nitrogen gas containing water vapor was then introduced into the IR reaction cell, and then spectra were collected every 10 min in the dark for a total of five acquisitions. Finally, to detect intermediates in the reaction, spectra were collected every 10 min under illumination for a total of five acquisitions.

2. Characterization

The crystal structure of the samples was analyzed on an X-ray diffractometer (ultimate IV, Rigaku) using Cu Ka radiation (λ = 0.15406 nm) in the range of 5-50. The scanning electron microscope (SEM) images of the catalysts were observed by Anfei Quantum 200 F electron microscope to clearly understand the morphology and structure of the catalysts. Transmission electron microscopy (TEM), higher-resolution transmission electron microscopy (HRTEM), and element mapping were performed using a JEOL model JEM2010 EX microscope at an accelerating voltage of 200 kV to further study the structure and elemental composition of the catalysts. X-ray photoelectron spectroscopy (XPS) results were received on a PHI Quantum 2000 XPS system with monochromatic Al Kα Radiation. Thermo gravimetry (TG) analysis was measured on a STA449F3 (Netzsch) instrument. The heating rate was set to 10°C min-1. The UV–vis diffuse reflectance spectra (UV-vis DRS) were recorded on a UV-vis spectrophotometer (Cary 500) to reveal the optical properties of the catalysts. The FTIR spectra were taken by a NICOLET IS50 Fourier transform infrared (FTIR) spectrometer. The Brunauer-Emmett-Teller (BET) specific surface areas of the samples were measured on a Micrometrics ASAP 2020 M volumetric gas sorption instrument by nitrogen adsorption/desorption isotherms at 77 K. The gas chromatography (GC-7890B, Agilent) equipped with a TCD, an FID detector, and a chromatographic column (MolSieve 5A) was used to measure the amount of generated O_2. The ion chromatography instrument (SH-CIC-100) was used to measure the concentration of

NH_4^+. The Steady-state photoluminescence (PL) and time-resolved PL decay spectra were measured on Fluorolog-3 type fluorescence spectrometer. (Test temperature: room temperature, light source: xenon lamp, detector: photomultiplier tube, excitation wavelength λ=360 nm). The average lifetime is calculated using the following formula: $\tau_{ave} = (A_1\tau_1^2+A_2\tau_2^2)/(A_1\tau_1+ A_2\tau_2)$. The Bruker EPR A300 spectrometer was used to record electron paramagnetic resonance (EPR) signals and analyze the active species during the reaction.

3. Electrochemical testing

Short-circuit photocurrent response, and Nyquist impedance measurements were tested on a CHI660D electrochemical workstation, respectively. The specific experimental process is as follows: the electrochemistry tests were carried out in a conventional three-electrode cell, including the working electrode, a Ptelectrode (counter electrode), and a saturated Ag/AgCl electrode (reference electrode). A clean fluorine-droped tin oxide (FTO) glass was used to prepare the working electrode. 5 mg of a sample was added into 0.5 mL of dimethyl formamide and dispersed uniformly by ultrasonication. The punched tape was used to create a groove on the surface of one end of the glass. Then, 20 μL of the solution mixture was dripped into this groove. After drying, insulated nail polish was used to cover the surface of the glass except for the groove and the other end of the glass. The three electrodes and the corresponding wiring of the electrochemical workstation were connected to carry out Short-circuit photocurrent response and Nyquist impedance measurement. The electrolytes for Nyquist impedance tests are 0.5 M $K_3[Fe(CN)_6]$ and while Short-circuit photocurrent response tests use 0.5 M Na_2SO_4 solution, respectively.

4. Isotopic labeling experiment

Isotope labeling experiments were performed using $^{15}N_2$ (98 atoms % ^{15}N) to trace the source of ammonium obtained. For 1H NMR measurements, the pH value of the sample solution was adjusted to 2 with hydrochloric acid and diluted with 20 % DMSO-

d6. The Measurements were performed on a Bruker Avance III HD 400.

5. Apparent Quantum Efficiency of Ammonia Production

Apparent quantum efficiency (AQE) was measured at ambient temperature using a 300w xenon lamp (Trustech, Beijing, PLS-SXE300c). The AQE was obtained by adding 80 mg MIL-101(Fe/Ni)-15% of to 20 mL of double deionized water in a glass reactor to irradiate an area of 4 cm^{-2}. The light was filtered through a 400 nm monochromatic filter with a bandwidth of ±15 nm, and the measured light intensity was 15.71 mW cm^{-2}, respectively. After 1 h of photocatalytic reaction, the yield of NH_4^+ was determined, and the mole number of ammonia molecules generated was 1.32 μmol. The detailed calculation method of AQE is as follows:

$$AQE(\%) = \frac{M \times N_A \times N_e}{\frac{P \times A \times t}{h \times v}} \times 100\%$$

Where M represents the molar number of generated ammonia molecules during the irradiation time t, and P, and A, are the incident light intensity, light incident area, and frequency, respectively; NA and h are the Avogadro's constant and Planck constant, respectively.

The calculation formula of AQE at 400 nm is as follows:

$$AQE(\%) = \frac{N_{reacted}}{N_{incident}} \times 100\% = \frac{M \times N_A \times N_e}{\frac{P \times A \times t}{h \times v}} \times 100\%$$

$$= \frac{M \times N_A \times N_e}{\frac{P \times A \times t \times \lambda}{h \times c}} \times 100\%$$

$$= \frac{1.32\mu mol \times 6.02 \times 10^{23} mol^{-1} \times 3}{\frac{15.71 mW\ cm^{-2} \times 4 cm^2 \times 3600 s \times 400 nm}{6.63 \times 10^{-34} Js \times 3 \times 10^{8} m\ s^{-1} d}} \times 100\%$$

$$= 0.53\%$$

6. Computational details

The density functional theory (DFT) calculations were performed by employing the universal generalized gradient correlation function and Vienna ab inition simulation

package (VASP5.4). A plane-wave basis set with a cutoff energy at 500 eV within the framework of the projector augmented wave method was adopted. The Gaussian smearing width was set to 0.2 eV. The Brillouin zone was sampled with a 3 × 3 × 1 K points. All atoms were allowed to converge to 0.01 eV $Å^{-1}$. The adsorption energy of N_2 molecule on catalyst is defined as:

$E = E_{tot} - E_{cat} – E_{N2}$

where E_{tot}, E_{cat} and E_{N2} demonstrate the total energies of catalyst with N_2 adsorption, catalyst before N_2 adsorption, and isolated N_2 molecule.

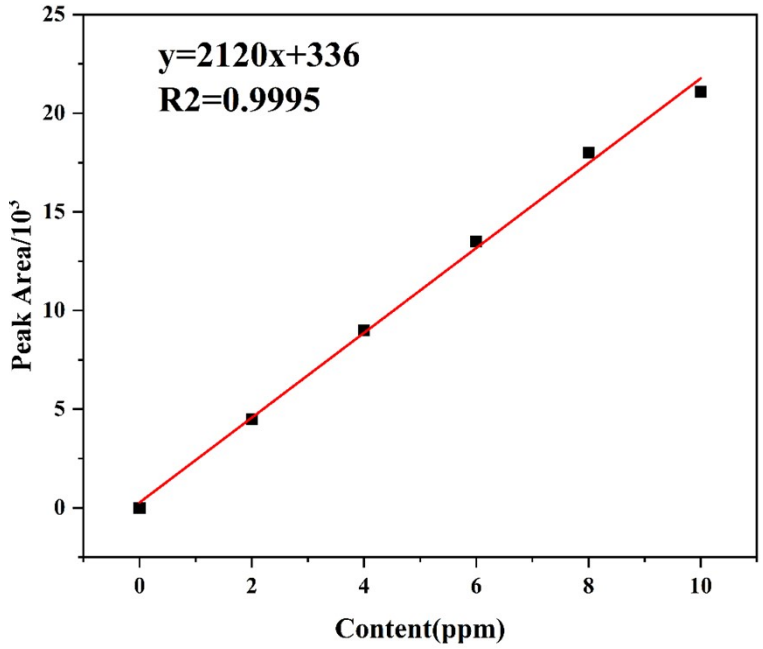

Fig.S1 The standard curves of NH_4^+ obtained from the Ion Chromatography.

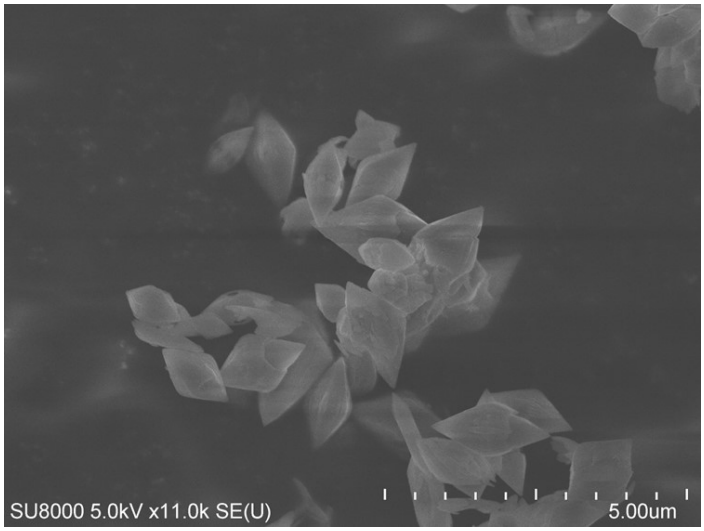

Fig. S2 SEM image of MIL-101(Fe).

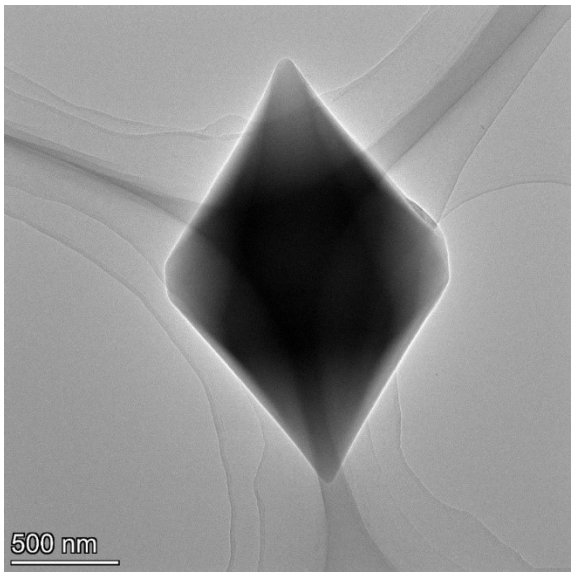

Fig. S3 TEM image of MIL-101(Fe).

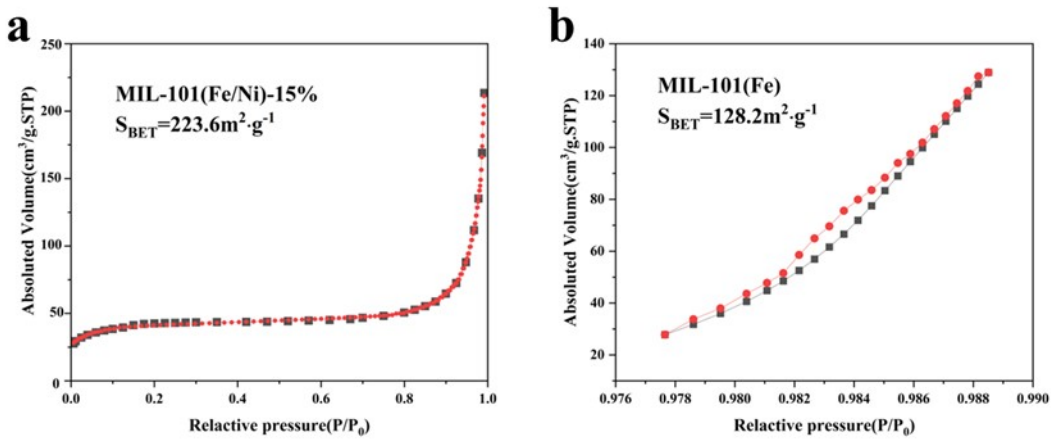

Fig. S4 N_2 sorption isotherms of the samples.

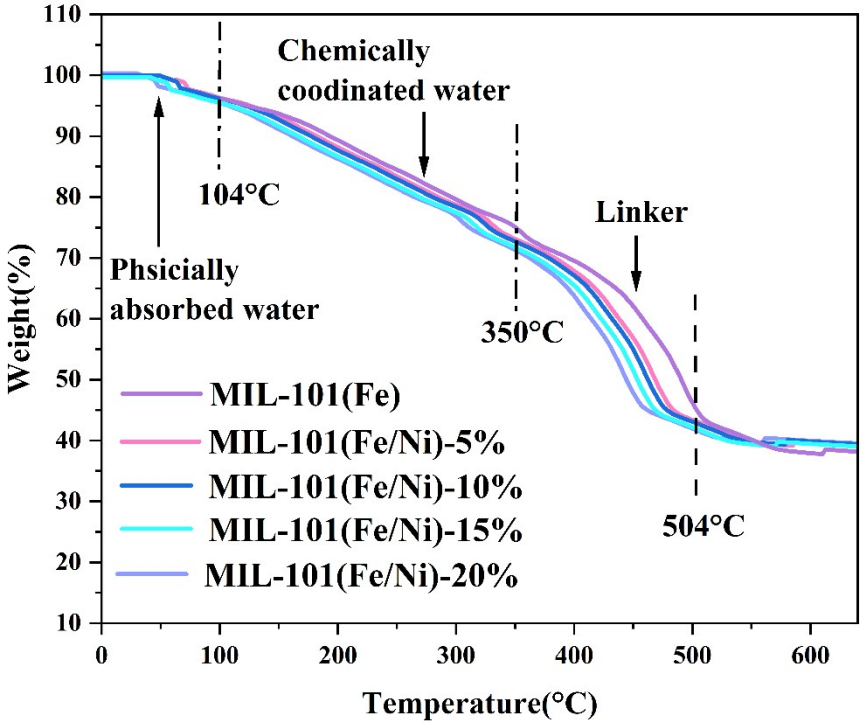

Fig. S5 TGA curves of the samples.

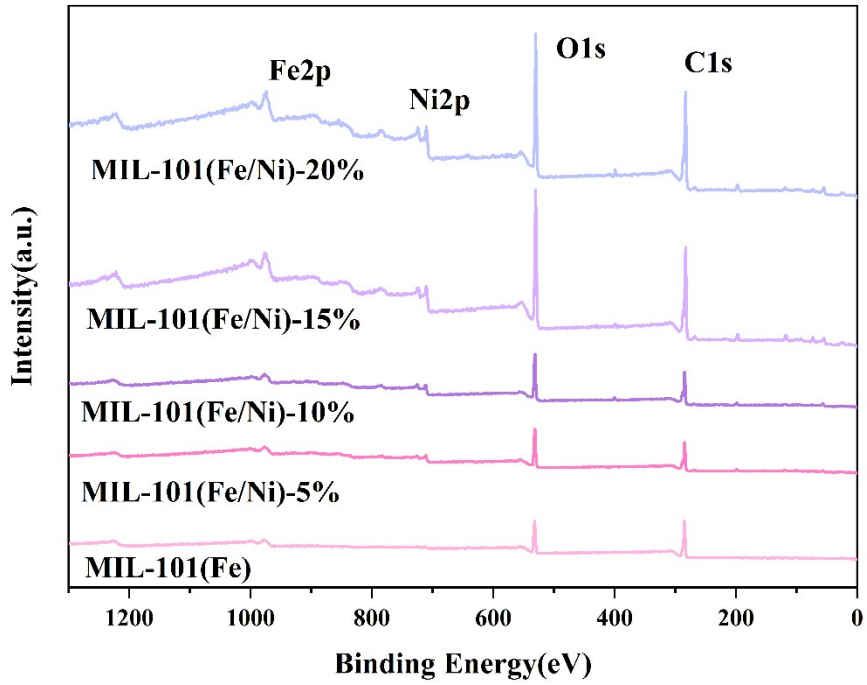

Fig. S6 XPS survey spectra of the prepared samples.

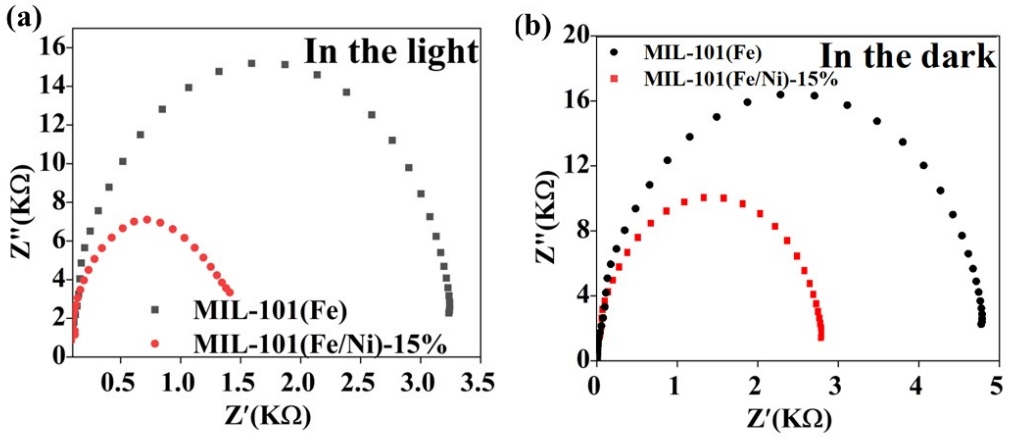

Fig. S7 Nyquist impedance plots in the light conditions(a), Nyquist impedance plots in the dark conditions(b).

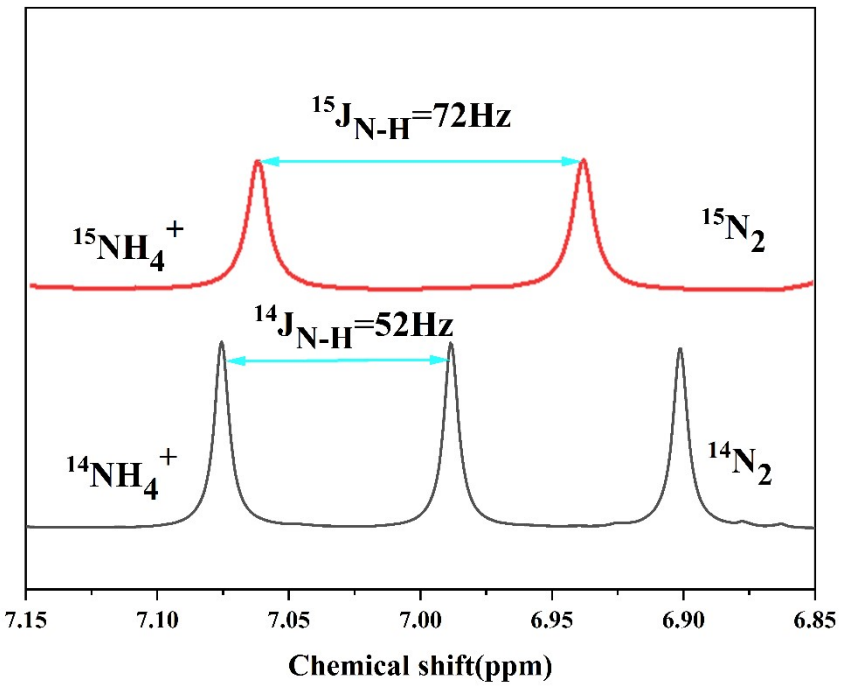

Fig. S8 (d) H-NMR spectra of NH_4^+ using MIL-101(Fe/Ni)-15% for the reduction of $^{14}N_2$ and $^{15}N_2$.

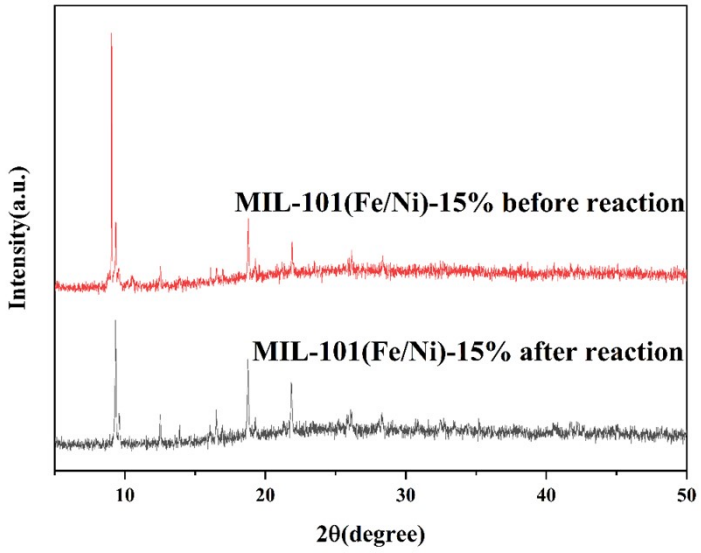

Fig. S9 XRD patterns of the MIL-101(Fe/Ni)-15% sample before and after reaction.

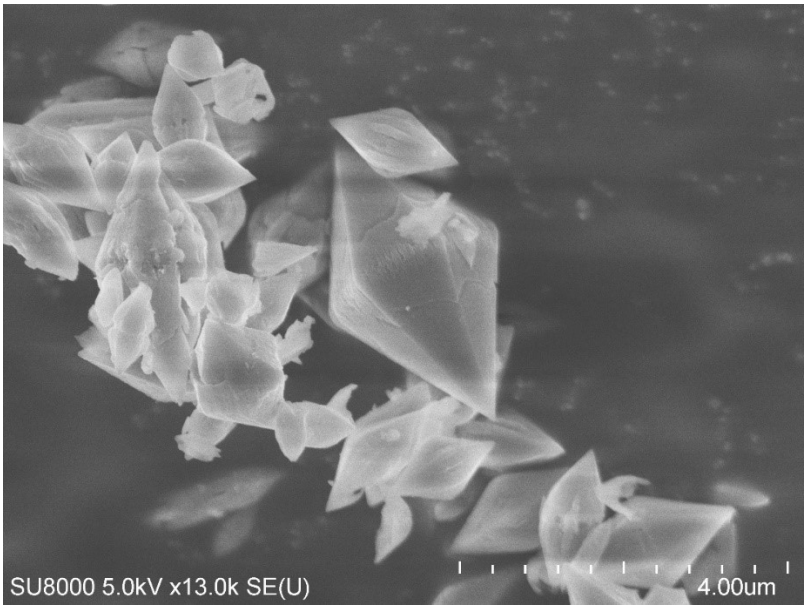

Fig. S10 SEM image of the MIL-101(Fe/Ni)-15% sample before and after reaction.

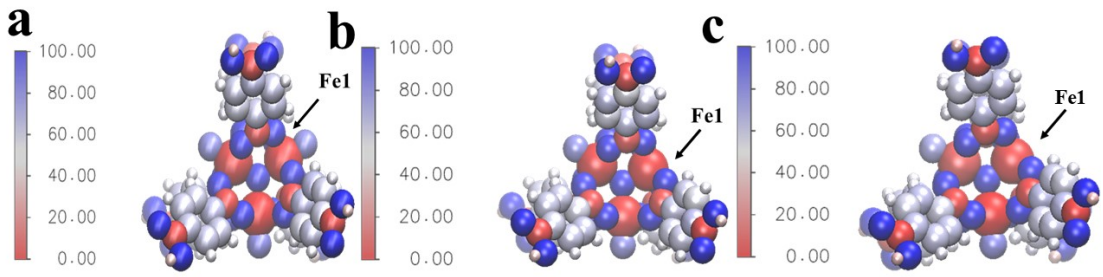

Fig. S11 Three structural models and computational N_2 adsorption energies (E_{Ads}) of pure MIL-101(Fe) (a), MIL-101(Fe) with OVs defects (MIL-101(Fe)-OVs, b), and Ni-doped MIL-101 (Fe) with Ni nearby OVs (Ni-MIL-101(Fe)-OVs, c).

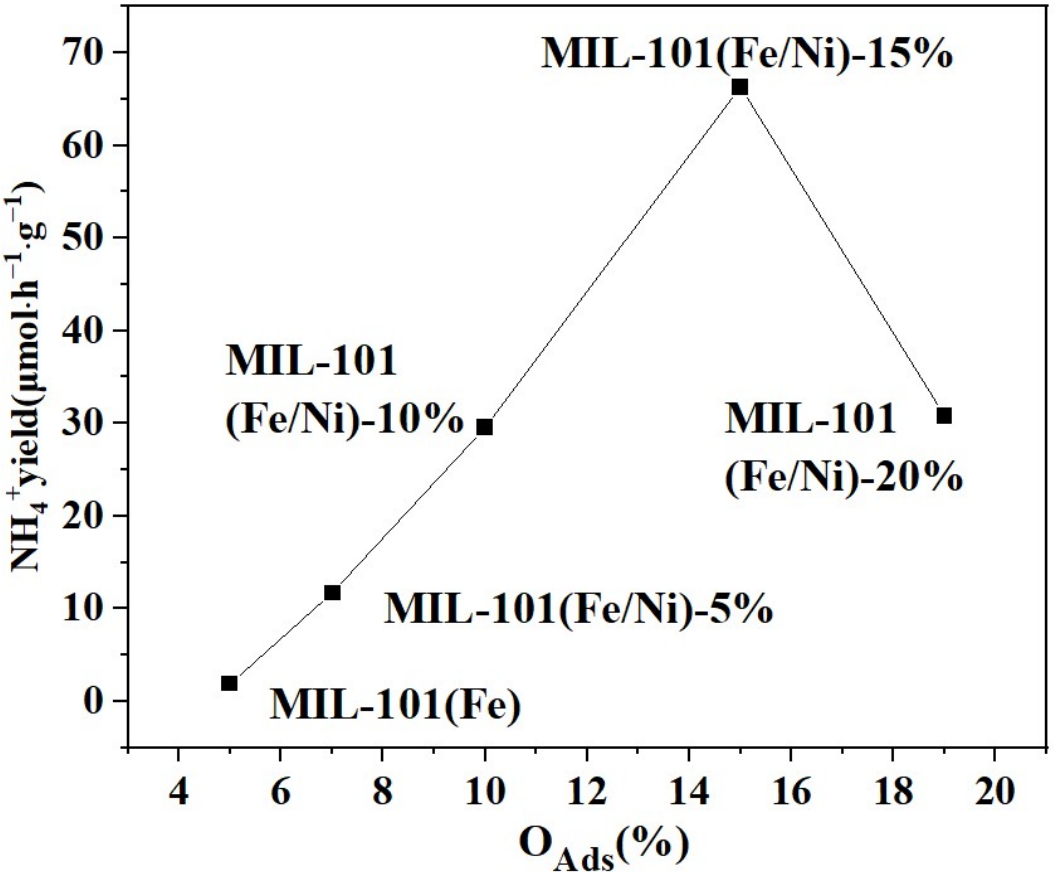

Fig. S12 Correlation plot between OV content and activity.

Table S1. Actual Ni content in MIL-101(Fe/Ni)-X% characterized by ICP

Catalyst	Theoretical ratio (Fe/Ni)	Actual ratio (Fe/Ni)
MIL-101 (Fe)	1:0	1:0
MIL-101 (Fe/Ni) -5%	0.95:0.05	0.97:0.03
MIL-101 (Fe/Ni) -10%	0.90:0.10	0.94:0.06
MIL-101 (Fe/Ni) -15%	0.85:0.15	0.89:0.11
MIL-101 (Fe/Ni) -20%	0.80:0.20	0.86:0.14

Table S2. The pore volume and pore size of the synthesized catalysts.

Catalyst	Pore volume (cm^3/ g)	Pore size (nm)
MIL-101(Fe)	0.54	2.8
MIL-101(Fe/Ni)-15%	0.38	2.5

Table S3. The ratio changes of loss weight for MIL-101(Fe/Ni)-X%.

Catalyst	The frist stage	The second stage	The third stage
MIL-101 (Fe)	3.2%	21.8%	57.7%
MIL-101 (Fe/Ni) -5%	3.2%	22.8%	57.9%
MIL-101 (Fe/Ni) -10%	3.2%	23.2%	58.6%
MIL-101 (Fe/Ni) -15%	3.2%	25.9%	58.7%
MIL-101 (Fe/Ni) -20%	3.2%	27.3%	59.0%

Table S4. Some reported MOFs-based photocatalysts in the system.

Catalyst	Scavenger	Measurement methods	NH_4^+ production rate	Ref.
MIL-101(Fe/Ni)-15%	None	Cationic chromatography	66.3μmol·h^{-1}·g^{-1}	This work
UiO-66$(SH)_2$	None	Cationic chromatography	32.28μmol·h^{-1}·g^{-1}	[47]
MIL68($Fe_{0.90}Cu_{0.10}$)	None	Cationic chromatography	21.0μmol·h^{-1}·g^{-1}	[24]
NH_2-ML-125(Ti)	Ethanol	Indophenol blue spectrophotometry	12.25μmol·h^{-1}·g^{-1}	[39]
Fe-abtc	K_2SO_3	Indophenol blue spectrophotometry	49.8μmol·h^{-1}·g^{-1}	[84]
Au@UiO-66	K_2SO_4	Nessler's reagent	18.9mmol·h^{-1}·g^{-1}	[38]
10%MoS_2/UiO-66$(SH)_2$	None	Cationic chromatography	54.08μmol·h^{-1}·g^{-1}	[45]
MIL-125(Ti)-250	None	Nessler's reagent	76.2 μmol·h^{-1}·g^{-1}	[46]
Chlor@UiO-66	None	Nessler's reagent	73.1μmol·h^{-1}· g^{-1}	[41]

Table S5. The Fe of charge of pure MIL-101(Fe).

	Charge	Valence electron	ΔCharge
Fe1	6.35	8.00	-1.65
Fe2	6.27	8.00	-1.73
Fe3	6.39	8.00	-1.61

Table S6. The Fe of charge of MIL-101(Fe)-OVs.

	Charge	Valence electron	ΔCharge
Fe1	6.27	8.00	-1.72
Fe2	6.36	8.00	-1.64
Fe3	6.34	8.00	-1.66

Table S7. The Fe and Ni of charge of Ni-MIL-101(Fe)-OVs.

	Charge	Valence electron	ΔCharge
Fe1	6.46	8.00	-1.54
Fe2	6.32	8.00	-1.68
Ni	8.64	8.00	-1.35